Journal of Engineering Physics and Thermophysics, Vol. 81, No. 4, 2008

MODELING OF VISCOELASTIC DEFORMATION OF IN-PLAN INHOMOGENEOUS THIN SLABS OF COMPLEX CONFIGURATION

K. S. Kurochka

UDC 539.37+519.6

A mathematical model, algorithm, and software for numerical simulation by the finite-element method of viscoelastic deformation of thin, inhomogeneous (in the horizontal plane) slabs having a geometrically complex boundary and (or) through vertical holes are presented. Using the software devised, the mathematical model developed has been investigated.

Many materials used in present-day town-building are capable of being deformed slowly in time at constant stresses. Such deformations may lead to a considerable change in the stressed–strained state of both the structural element and the entire structure as a whole, which undoubtedly will influence the durability and functionality of these elements and structures.

In erecting buildings and structures, wide use is made of such a structural element as the slab, e.g., in laying flexible foundations or disks for the floors of buildings [1]. Below, the problem of simulation of the viscoelastic stressed–strained state of slabs that are inhomogeneous in the horizontal plane and have a geometrically complex boundary and (or) through vertical holes is considered. It is assumed that the ratio of the characteristic dimension of the slab in plan to its thickness lies within 10–100. Consequently, to determine the stressed–strained state of a slab one can make use of the theory of bending of thin plates which is based on the Kirchhoff hypotheses [1, 2]:

(1) the slab thickness does not change in deformation;

(2) after the bending of the slab the normal to its middle plane is preserved;

(3) on application of loading all the points of the middle plane do not move along the X and Y axes;

(4) the stresses caused by the pressing of the horizontal layers of the slab on one another can be neglected.

Moreover, the Cauchy equations are valid [2]:

$$\varepsilon_x = \frac{\partial u}{\partial x}, \quad \varepsilon_y = \frac{\partial v}{\partial y}, \quad \varepsilon_z = \frac{\partial w}{\partial z}, \quad \gamma_{xy} = \frac{\partial u}{\partial y} + \frac{\partial v}{\partial x}, \quad \gamma_{yz} = \frac{\partial u}{\partial z} + \frac{\partial w}{\partial y}, \quad \gamma_{zx} = \frac{\partial u}{\partial z} + \frac{\partial w}{\partial x}. \tag{1}$$

From the first Kirchhoff hypothesis it follows that the deformations

$$\varepsilon_z = 0. \tag{2}$$

Substituting (2) into (1), we obtain $\varepsilon_z = \partial w/\partial z = 0$; consequently, the deflection of the slab is independent of z, i.e., $w = w(x, y)$.

From the second hypothesis it follows that the rectangle formed along the Z and X or Z and Y axes will not change, i.e., the tangential deformations

$$\gamma_{yz} = 0 \quad \text{and} \quad \gamma_{zx} = 0. \tag{3}$$

Using (3), from Eq. (1) we may obtain that $\gamma_{yz} = \partial v/\partial z + \partial w/\partial y = 0$ and $\gamma_{zx} = \partial w/\partial x + \partial u/\partial z = 0$. Consequently, $\partial v/\partial z = -\partial w/\partial y$ and $\partial u/\partial z = -\partial w/\partial x$. Carrying out integration over z, we have

P. O. Sukhoi Gomel State Technical University, 48 Oktyabr' Ave., Gomel, 246746, Belarus; email: Kurochka@gstu.gomel.by. Translated from Inzhenerno-Fizicheskii Zhurnal, Vol. 81, No. 4, pp. 778–788, July–August, 2008. Original article submitted December 22, 2006; revision submitted October 9, 2007.

$$u = -z\frac{\partial w}{\partial x} + f_1(x, y), \quad v = -z\frac{\partial w}{\partial y} + f_2(x, y), \tag{4}$$

where $f_1(x, y)$ and $f_2(x, y)$ are arbitrary functions.

According to the third hypothesis of Kirchhoff for the middle plane, i.e., at $z = 0$, we obtain $u_0 = 0$ and $v_0 = 0$, whence $u_0 = f_1(x, y) = 0$ and $v_0 = f_2(x, y) = 0$. Thus, we represent (4) as follows:

$$u = -z\frac{\partial w}{\partial x}, \quad v = -z\frac{\partial w}{\partial y}. \tag{5}$$

According to the foregoing, the Cauchy equations (1) for a thin slab are transformed to give

$$\varepsilon_x = -z\frac{\partial^2 w}{\partial x^2}, \quad \varepsilon_y = -z\frac{\partial^2 w}{\partial y^2}, \quad \gamma_{xy} = -2z\frac{\partial^2 w}{\partial x \partial y}. \tag{6}$$

From the fourth hypothesis it follows that the stresses along the Z axis

$$\sigma_z = 0. \tag{7}$$

Consequently, the vectors of deformations and stresses will have three nonzero components each: $\varepsilon = \{\varepsilon_x \varepsilon_y \gamma_{xy}\}$ and $\sigma = \{\sigma_x \sigma_y \tau_{xy}\}$, i.e., the Hooke law [1, 2] for a thin slab can be rewritten as follows:

$$\begin{Bmatrix} \sigma_x \\ \sigma_y \\ \tau_{xy} \end{Bmatrix} = \frac{E}{1-\mu^2} \begin{bmatrix} 1 & \mu & 0 \\ \mu & 1 & 0 \\ 0 & 0 & \dfrac{1-\mu}{2} \end{bmatrix} \begin{Bmatrix} \varepsilon_x \\ \varepsilon_y \\ \gamma_{xy} \end{Bmatrix}. \tag{8}$$

Viscoelastic Deformation of a Thin Slab. To describe the process of viscoelastic deformation of a thin slab, we will use the Boltzmann–Volterra linear theory of hereditary creep [2], according to which for viscoelastic bodies the following relations hold:

$$\begin{aligned} \sigma_x(t) &= 2G(t)(1 - \Gamma_{sh})[\varepsilon_x(t) - \varepsilon_{av}(t)] + 3K(t)(1 - \Gamma_{vol})\varepsilon_{av}(t), \\ \sigma_y(t) &= 2G(t)(1 - \Gamma_{sh})[\varepsilon_y(t) - \varepsilon_{av}(t)] + 3K(t)(1 - \Gamma_{vol})\varepsilon_{av}(t), \\ \sigma_z(t) &= 2G(t)(1 - \Gamma_{sh})[\varepsilon_z(t) - \varepsilon_{av}(t)] + 3K(t)(1 - \Gamma_{vol})\varepsilon_{av}(t), \\ \tau_{xy}(t) &= G(t)(1 - \Gamma_{sh})\gamma_{xy}(t), \ldots, \end{aligned} \tag{9}$$

where $\varepsilon_{av}(t) = [\varepsilon_x(t) + \varepsilon_y(t) + \varepsilon_z(t)]/3$.

In a scalar form, Eq. (9) is

$$\begin{aligned} \sigma_x(t) &= 2G(t)[\varepsilon_x(t) - \varepsilon_{av}(t)] - 2\int_0^t \Gamma_{sh}(t, \xi)[\varepsilon_x(\xi) - \varepsilon_{av}(\xi)]\,d\xi + 3K(t)\varepsilon_{av}(t) - 3\int_0^t \Gamma_{vol}(t, \xi)\varepsilon_{av}(\xi)\,d\xi, \\ \sigma_y(t) &= 2G(t)[\varepsilon_y(t) - \varepsilon_{av}(t)] - 2\int_0^t \Gamma_{sh}(t, \xi)[\varepsilon_y(\xi) - \varepsilon_{av}(\xi)]\,d\xi + 3K(t)\varepsilon_{av}(t) - 3\int_0^t \Gamma_{vol}(t, \xi)\varepsilon_{av}(\xi)\,d\xi, \\ \sigma_z(t) &= 2G(t)[\varepsilon_z(t) - \varepsilon_{av}(t)] - 2\int_0^t \Gamma_{sh}(t, \xi)[\varepsilon_z(\xi) - \varepsilon_{av}(\xi)]\,d\xi + 3K(t)\varepsilon_{av}(t) - 3\int_0^t \Gamma_{vol}(t, \xi)\varepsilon_{av}(\xi)\,d\xi, \end{aligned} \tag{10}$$

$$\tau_{xy}(t) = G(t)\,\gamma_{xy}(t) - \int_0^t \Gamma_{sh}(t,\xi)\,\gamma_{xy}(\xi)\,d\xi, \ldots .$$

We assume that in viscoelastic deformation the volumetric deformations will be elastic, i.e., $K(t)(1-\Gamma_{vol}) \equiv K(t)$. Then, taking into account Eqs. (2), (3), and (7) and expressing the shear modulus $G(t)$ and the volumetric deformation modulus $K(t)$ in terms of the Young modulus $E(t)$ and Poisson coefficient $\mu(t)$, we can write relation (9) as

$$\begin{aligned}
\sigma_x(t) &= \frac{E(t)}{1+\mu(t)}(1-\Gamma_{sh})[\varepsilon_x(t)-\varepsilon_{av}(t)] + \frac{E(t)}{1-\mu(t)}\varepsilon_{av}(t), \\
\sigma_y(t) &= \frac{E(t)}{1+\mu(t)}(1-\Gamma_{sh})[\varepsilon_y(t)-\varepsilon_{av}(t)] + \frac{E(t)}{1-\mu(t)}\varepsilon_{av}(t), \\
\tau_{xy}(t) &= \frac{E(t)}{2(1+\mu(t))}(1-\Gamma_{sh})\gamma_{xy}(t).
\end{aligned} \tag{11}$$

Let us consider the first equation of (11) taking into account that $\varepsilon_{av}(t) = [\varepsilon_x(t) + \varepsilon_y(t)]/2$:

$$\sigma_x(t) = \frac{E(t)}{2(1+\mu(t))}(1-\Gamma_{sh})[\varepsilon_x(t)-\varepsilon_y(t)] + \frac{E(t)}{2(1-\mu(t))}[\varepsilon_x(t)+\varepsilon_y(t)],$$

whence

$$\sigma_x(t) = \frac{E(t)}{1-\mu(t)^2}[\varepsilon_x(t)+\mu(t)\varepsilon_y(t)] - \frac{E(t)}{2(1+\mu(t))}\Gamma_{sh}[\varepsilon_x(t)-\varepsilon_y(t)].$$

Having performed analogous transformations for the remaining components of the stress vector, we can rewrite Eq. (11) as

$$\begin{aligned}
\sigma_x(t) &= \frac{E(t)}{1-\mu(t)^2}[\varepsilon_x(t)+\mu(t)\varepsilon_y(t)] - \frac{E(t)}{2(1+\mu(t))}\Gamma_{sh}[\varepsilon_x(t)-\varepsilon_y(t)], \\
\sigma_y(t) &= \frac{E(t)}{1-\mu(t)^2}[\mu(t)\varepsilon_x(t)+\varepsilon_y(t)] - \frac{E(t)}{2(1+\mu(t))}\Gamma_{sh}[-\varepsilon_x(t)+\varepsilon_y(t)], \\
\tau_{xy}(t) &= \frac{E(t)}{1-\mu(t)^2}\frac{1-\mu(t)}{2}\gamma_{xy}(t) - \frac{E(t)}{2(1+\mu(t))}\Gamma_{sh}\gamma_{xy}(t).
\end{aligned} \tag{12}$$

In a scalar form the first relation in (12) will be expressed as

$$\sigma_x(t) = \frac{E(t)}{1-\mu(t)^2}\Big(\varepsilon_x(t)+\mu(t)\varepsilon_y(t)\Big) - \frac{E(t)}{2(1+\mu(t))}\left(\frac{2(1+\mu(t))}{E(t)}\int_0^t \Gamma_{sh}(t,\xi)\Big(\varepsilon_x(\xi)-\varepsilon_y(\xi)\Big)d\xi\right)$$

or

$$\sigma_x(t) = \frac{E(t)}{1-\mu(t)^2}\Big[\varepsilon_x(t)+\mu(t)\varepsilon_y(t)\Big] - \left[\int_0^t \Gamma_{sh}(t,\xi)\varepsilon_x(\xi)\,d\xi - \int_0^t \Gamma_{sh}(t,\xi)\varepsilon_y(\xi)\,d\xi\right]. \tag{13}$$

Let us consider the integral from expression (13):

$$I = \int_0^t \Gamma_{sh}(t, \xi)\, \varepsilon(\xi)\, d\xi .$$

We will divide the time interval [0, t] into n intervals; then

$$I = \int_0^t \Gamma_{sh}(t, \xi)\, \varepsilon(\xi)\, d\xi = \sum_{j=0}^{n-1} \int_{t_j}^{t_{j+1}} \Gamma_{sh}(t, \xi)\, \varepsilon(\xi)\, d\xi .$$

According to the theorem of the mean, we obtain

$$I = \sum_{j=0}^{n-1} \varepsilon(\eta) \int_{t_j}^{t_{j+1}} \Gamma_{sh}(t, \xi)\, d\xi , \quad \eta \in [t_j; t_{j+1}] .$$

As the point η, we will approximately take one of the limits of the interval, say, t_j:

$$I \approx \sum_{j=0}^{n-1} \varepsilon(t_j) \int_{t_j}^{t_{j+1}} \Gamma_{sh}(t, \xi)\, d\xi , \tag{14}$$

where

$$I = \lim_{n\to\infty} \sum_{j=0}^{n-1} \left[\varepsilon(t_j) \int_{t_j}^{t_{j+1}} \Gamma_{sh}(t, \xi)\, d\xi \right].$$

We will take the relaxation kernel in the form [2, 3]

$$\Gamma_{sh}(t, \xi) = \delta G \exp(-\delta_1 (t - \xi)) . \tag{15}$$

Substituting (15) into (14) and integrating, we obtain

$$I \approx \sum_{j=0}^{n-1} \varepsilon(t_j) \int_{t_j}^{t_{j+1}} \delta G \exp(-\delta_1 (t - \xi))\, d\xi = \frac{\delta}{\delta_1} G \sum_{j=0}^{n-1} \left[\varepsilon(t_j) \left[\exp(-\delta_1 (t - t_{j+1})) - \exp(-\delta_1 (t - t_j)) \right] \right]. \tag{16}$$

In case the relaxation kernel, $\Gamma_{sh}(t, \xi)$ will be prescribed in another form [2]; then integration in (16) can be performed numerically.

Using expression (16), we can rewrite relation (13) as

$$\sigma_x(t) = \frac{E(t)}{1 - \mu(t)^2} [\varepsilon_x(t) + \mu(t)\, \varepsilon_y(t)] - \frac{\delta}{\delta_1} G \left[\sum_{j=0}^{n-1} \varepsilon_x(t_j) \left[\exp(-\delta_1 (t - t_{j+1})) - \exp(-\delta_1 (t - t_j)) \right] \right.$$

$$\left. - \sum_{j=0}^{n-1} \varepsilon_y(t_j) \left[\exp(-\delta_1 (t - t_{j+1})) - \exp(-\delta_1 (t - t_j)) \right] \right]. \tag{17}$$

We will consider the last term of (17). For the initial time $t = 0$ it will be equal to 0, for the time t_1 — to $\frac{\delta}{\delta_1} G[\varepsilon_x(t_1)[1 - \exp(-\delta_1(t_1 - t_0))] - \varepsilon_y(t_1)[1 - \exp(-\delta_1(t_1 - t_0))]]$, for the time t_m — to $\frac{\delta}{\delta_1} G\left[\sum_{j=0}^{m-1} \varepsilon_x(t_j)[\exp(-\delta_1(t_m - t_{j+1})) - \exp(-\delta_1(t_m - t_j))] - \sum_{j=0}^{m-1} \varepsilon_y(t_j)[\exp(-\delta_1(t_m - t_{j+1})) - \exp(-\delta_1(t_m - t_j))]\right]$. Thus, for an arbitrary instant of time t_{j+1} relations (12) take the form

$$\sigma_x(t_{i+1}) = \frac{E(t_{i+1})}{1 - \mu(t)^2}[\varepsilon_x(t_{i+1}) + \mu(t)\,\varepsilon_y(t_{i+1})]$$

$$-\frac{\delta}{\delta_1} G \sum_{j=0}^{i} \left[\left[\exp(-\delta_1(\varepsilon(t_{i+1} - t_{j+1})) - \exp(-\delta_1(t_{i+1} - t_j))\right][\varepsilon_x(t_j) - \varepsilon_y(t_j)]\right],$$

$$\sigma_y(t_{i+1}) = \frac{E(t_{i+1})}{1 - \mu(t)^2}[\mu(t)\,\varepsilon_x(t_{i+1}) + \varepsilon_y(t_{i+1})] \tag{18}$$

$$-\frac{\delta}{\delta_1} G \sum_{j=0}^{i} \left[\left[\exp(-\delta_1(t_{i+1} - t_{j+1})) - \exp(-\delta_1(t_{i+1} - t_j))\right][-\varepsilon_x(t_j) + \varepsilon_y(t_j)]\right],$$

$$\tau_{xy}(t_{i+1}) = \frac{E(t)}{1 - \mu(t)^2}\frac{1 - \mu(t)}{2}\gamma_{xy}(t_{i+1}) - \frac{\delta}{\delta_1} G \sum_{j=0}^{i} \left[\left[\exp(-\delta_1(t_{i+1} - t_{j+1})) - \exp(-\delta_1(t_{i+1} - t_j))\right]\gamma_{xy}(t_i)\right].$$

Investigation of the Mathematical Model by the Finite-Element Method. To take into account the complex geometry, the presence of through holes, and the inhomogeneous properties of the slabs considered, it is worthwhile to use the method of finite elements. By assigning different properties to finite elements, it is possible to take into account the majority of the structural features of the slab. Moreover, the application of finite elements of small enough dimensions makes it possible to approximate, with an accuracy sufficient for practice, the slabs that have geometrically complex boundaries and an in-plan inhomogeneous structure.

The adoption of the Kirchhoff hypotheses in investigation of the stressed–strained state of slabs allows one to use plane finite elements for approximation [4], which ultimately makes it possible to considerably reduce the number of computations in computer simulation.

We will rewrite expressions (18) in a matrix form:

$$\boldsymbol{\sigma}_{i+1} = [\mathbf{E}]_{i+1}\,\boldsymbol{\varepsilon}_{i+1} - \frac{\delta}{\delta_1} G \sum_{j=0}^{i} \left([\mathbf{S}]_{ji}\,\boldsymbol{\varepsilon}_j\right), \tag{19}$$

where

$$[\mathbf{E}]_{i+1} = \frac{E(t_{i+1})}{1 - \mu(t)^2}\begin{bmatrix} 1 & \mu(t) & 0 \\ \mu(t) & 1 & 0 \\ 0 & 0 & \dfrac{1 - \mu(t)}{2} \end{bmatrix};\quad [\mathbf{S}]_{ji} = \left[\exp\left(-\delta_1\left(t_{i+1} - t_{j+1}\right)\right) - \exp\left(-\delta_1\left(t_{i+1} - t_j\right)\right)\right]\begin{bmatrix} 1 & -1 & 0 \\ -1 & 1 & 0 \\ 0 & 0 & 1 \end{bmatrix}.$$

Consequently, to find a viscoelastic stressed–strained state of a thin slab it is necessary to know the entire prehistory of deformation, i.e., the deformations ε_0, ε_1, ε_2, ... In the initial instant of time, the deformation of the slab can be found from the solution of an elastic problem.

We assume that at any arbitrary fixed instant of time we will have a linear stressed state. Then, the deformation energy density will be expressed in terms of the area of the diagram of material deformation:

$$U^0(t_{i+1}) = \int_0^{\varepsilon_{\text{int}}(t_{i+1})} \sigma_{\text{int}} d\varepsilon_{\text{int}},$$

where

$$\varepsilon_{\text{int}} = \frac{\sqrt{2}}{3}\sqrt{(\varepsilon_x - \varepsilon_y)^2 + (\varepsilon_y - \varepsilon_z)^2 + (\varepsilon_z - \varepsilon_x)^2 + 6(\gamma_{xy}^2 + \gamma_{yz}^2 + \gamma_{zx}^2)};$$

$$\sigma_{\text{int}} = \frac{1}{\sqrt{2}}\sqrt{(\sigma_x - \sigma_y)^2 + (\sigma_y - \sigma_z)^2 + (\sigma_z - \sigma_x)^2 + 6(\tau_{xy}^2 + \tau_{yz}^2 + \tau_{zx}^2)}.$$

For one finite element the deformation energy is

$$U_{i+1} = \iiint_V U^0(t_{i+1}) dV.$$

Then, according to the adopted hypothesis and in conformity with the principle of possible displacements, for the instant of time t_{i+1} we will have [1, 2]

$$\left(\tilde{\mathbf{g}}_{i+1}^{\text{n}}\right)^{\text{tr}} \mathbf{R} = \iiint_V \tilde{\varepsilon}_{i+1}^{\text{tr}}\, \sigma_{i+1} dV, \tag{20}$$

where the tilde denotes variation.

We will consider a rectangular finite element in bending strain under the action of lateral loading [1, 2, 4]. For bending slabs the Kirchhoff hypotheses (2), (3), (5), and (7) are valid so that each node will have three degrees of freedom:

$$\left(\mathbf{g}^{\text{n}}\right)^{\text{tr}} = \{w \;\; \theta_x \;\; \theta_y\}, \quad \theta_x = \frac{\partial w}{\partial y}; \quad \theta_y = \frac{\partial w}{\partial x}.$$

To express the surface of deflection a polynomial that satisfies the homogeneous differential equation of a bending slab [4] is adopted:

$$w(x, y) = \alpha_1 + \alpha_2 x + \alpha_3 y + \alpha_4 x^2 + \alpha_5 y^2 + \alpha_6 xy + \alpha_7 x^2 y + \alpha_8 xy^2 + \alpha_9 x^3 + \alpha_{10} y^3 + \alpha_{11} x^3 y + \alpha_{12} xy^3. \tag{21}$$

Differentiating (21), we obtain

$$\mathbf{g} = [\mathbf{A}]\,\boldsymbol{\alpha}, \tag{22}$$

where

$$[\mathbf{A}] = \begin{bmatrix} 1 & x & y & x^2 & y^2 & xy & x^2y & xy^2 & x^3 & y^3 & x^3y & xy^3 \\ 0 & 1 & 0 & 2x & 0 & y & 2xy & y^2 & 3x^2 & 0 & 3x^2y & y^3 \\ 0 & 0 & 1 & 0 & 2y & x & x^2 & 2xy & 0 & 3y^2 & x^3 & 3xy^2 \end{bmatrix}.$$

Since (22) takes place for any point of the finite element, for its apices we will have

$$\mathbf{g}^{\mathrm{n}} = [\mathbf{B}]\,\boldsymbol{\alpha}\,, \tag{23}$$

where

$$[\mathbf{B}] = \begin{bmatrix}
1 & x_1 & y_1 & x_1^2 & y_1^2 & x_1y_1 & x_1^2y_1 & x_1y_1^2 & x_1^3 & y_1^3 & x_1^3y_1 & x_1y_1^3 \\
0 & 1 & 0 & 2x_1 & 0 & y_1 & 2x_1y_1 & y_1^2 & 3x_1^2 & 0 & 3x_1^2y_1 & y_1^3 \\
0 & 0 & 1 & 0 & 2y_1 & x_1 & x_1^2 & 2x_1y_1 & 0 & 3y_1^2 & x_1^3 & 3x_1y_1^2 \\
1 & x_2 & y_2 & x_2^2 & y_2^2 & x_2y_2 & x_2^2y_2 & x_2y_2^2 & x_2^3 & y_2^3 & x_2^3y_2 & x_2y_2^3 \\
0 & 1 & 0 & 2x_2 & 0 & y_2 & 2x_2y_2 & y_2^2 & 3x_2^2 & 0 & 3x_2^2y_2 & y_2^3 \\
0 & 0 & 1 & 0 & 2y_2 & x_2 & x_2^2 & 2x_2y_2 & 0 & 3y_2^2 & x_2^3 & 3x_2y_2^2 \\
1 & x_3 & y_3 & x_3^2 & y_3^2 & x_3y_3 & x_3^2y_3 & x_3y_3^2 & x_3^3 & y_3^3 & x_3^3y_3 & x_3y_3^3 \\
0 & 1 & 0 & 2x_3 & 0 & y_3 & 2x_3y_3 & y_3^2 & 3x_3^2 & 0 & 3x_3^2y_3 & y_3^3 \\
0 & 0 & 1 & 0 & 2y_3 & x_3 & x_3^2 & 2x_3y_3 & 0 & 3y_3^2 & x_3^3 & 3x_3y_3^2 \\
1 & x_4 & y_4 & x_4^2 & y_4^2 & x_4y_4 & x_4^2y_4 & x_4y_4^2 & x_4^3 & y_4^3 & x_4^3y_4 & x_4y_4^3 \\
0 & 1 & 0 & 2x_4 & 0 & y_4 & 2x_4y_4 & y_4^2 & 3x_4^2 & 0 & 3x_4^2y_4 & y_4^3 \\
0 & 0 & 1 & 0 & 2y_4 & x_4 & x_4^2 & 2x_4y_4 & 0 & 3y_4^2 & x_4^3 & 2x_4y_4^2
\end{bmatrix};$$

x_i, y_i, z_i ($i = \overline{1,4}$) are the coordinates of the nodes of the finite element.

From Eq. (23) it follows that

$$\boldsymbol{\alpha} = [\mathbf{B}]^{-1}\,\mathbf{g}^{\mathrm{n}}\,. \tag{24}$$

Using the Cauchy equation (6) and having differentiated Eq. (21), we obtain

$$\boldsymbol{\varepsilon} = -\,z\,[\mathbf{C}]\,\boldsymbol{\alpha}\,, \tag{25}$$

where

$$[\mathbf{C}] = \begin{bmatrix}
0 & 0 & 0 & 2 & 0 & 0 & 2y & 0 & 6x & 0 & 6xy & 0 \\
0 & 0 & 0 & 0 & 2 & 0 & 0 & 2x & 0 & 6y & 0 & 6xy \\
0 & 0 & 0 & 0 & 0 & 2 & 4x & 4y & 0 & 0 & 6x^2 & 6y^2
\end{bmatrix}.$$

The substitution of (24) into (25) yields

$$\boldsymbol{\varepsilon} = -\,z\,[\mathbf{C}]\,[\mathbf{B}]^{-1}\,\mathbf{g}^{\mathrm{n}}\,. \tag{26}$$

Using (26), we may write (19) as

$$\boldsymbol{\sigma}_{i+1} = -\,z\,[\mathbf{E}]_{i+1}\,[\mathbf{C}]\,[\mathbf{B}]^{-1}\,\mathbf{g}^{\mathrm{n}}_{i+1} + z\,\frac{\delta}{\delta_1}\,G\sum_{j=0}^{i}\left([\mathbf{S}]_{ji}\,[\mathbf{C}]\,[\mathbf{B}]^{-1}\,\mathbf{g}^{\mathrm{n}}_{j}\right). \tag{27}$$

The principle of possible displacements (20) for the finite element considered will have the form

$$\left(\tilde{\mathbf{g}}^{\mathrm{n}}_{i+1}\right)^{\mathrm{tr}}\mathbf{R} = \int_0^b\int_0^a\int_{-\frac{h}{2}}^{\frac{h}{2}} \tilde{\boldsymbol{\varepsilon}}^{\mathrm{tr}}_{i+1}\,\boldsymbol{\sigma}_{i+1}\,dV\,. \tag{28}$$

We substitute (26) and (27) into (28) to obtain

$$\left(\tilde{\mathbf{g}}_{i+1}^{\mathrm{n}}\right)^{\mathrm{tr}} \mathbf{R} = \int_0^b \int_0^a \int_{-\frac{h}{2}}^{\frac{h}{2}} z \left(\tilde{\mathbf{g}}_{i+1}^{\mathrm{n}}\right)^{\mathrm{tr}} [\mathbf{B}]^{-1^{\mathrm{tr}}} [\mathbf{C}]^{\mathrm{tr}} z \left([\mathbf{E}]_{i+1} [\mathbf{C}] [\mathbf{B}]^{-1} \mathbf{g}_{i+1}^{\mathrm{n}} - \frac{\delta}{\delta_1} G \sum_{j=0}^{i} \left([\mathbf{S}]_{ji} [\mathbf{C}] [\mathbf{B}]^{-1} \mathbf{g}_j^{\mathrm{n}} \right) \right) dz\, dx\, dy .$$

Since the matrix [**B**] and the vector of nodal displacements $\mathbf{g}^{\mathrm{n}}$ are independent of the coordinates, they can be taken out of the integral. Then, having integrated the latter relation over z, we obtain

$$\mathbf{R} = \frac{h^3}{12} [\mathbf{B}]^{-1^{\mathrm{tr}}} \left(\int_0^a \int_0^b [\mathbf{C}]^{\mathrm{tr}} [\mathbf{E}]_{i+1} [\mathbf{C}]\, dx\, dy \right) [\mathbf{B}]^{-1} \mathbf{g}_{i+1}^{\mathrm{n}} - \mathbf{R}_{i+1}^{\mathrm{vis}} , \tag{29}$$

where

$$\mathbf{R}_{i+1}^{\mathrm{vis}} = \frac{h^3}{12} \frac{\delta}{\delta_1} G \sum_{j=0}^{i} \Bigg((\exp(-\delta_1 (t_{i+1} - t_{j+1})) - \exp(-\delta_1 (t_{i+1} - t_j)))$$

$$\times [\mathbf{B}]^{-1^{\mathrm{tr}}} \left(\int_0^a \int_0^b [\mathbf{C}]^{\mathrm{tr}} \begin{bmatrix} 1 & -1 & 0 \\ -1 & 1 & 0 \\ 0 & 0 & 1 \end{bmatrix} [\mathbf{C}]\, dx\, dy \right) [\mathbf{B}]^{-1} \mathbf{g}_j^{\mathrm{n}} \Bigg). \tag{30}$$

Moreover, the values of the integrals in (29) and (30) can easily be calculated exactly.

Expression (29) can be rewritten in the form

$$\mathbf{R}_{i+1}^{\mathrm{act}} = [\mathbf{K}]_{i+1} \mathbf{g}_{i+1}^{\mathrm{n}} , \tag{31}$$

where $[\mathbf{K}]_{i+1} = \frac{h^3}{12} [\mathbf{B}]^{-1^{\mathrm{tr}}} \left(\int_0^a \int_0^b [\mathbf{C}]^{\mathrm{tr}} [\mathbf{E}]_{i+1} [\mathbf{C}] dx dy \right) [\mathbf{B}]^{-1}$ is the matrix of the rigidity of the finite element:

$$\mathbf{R}_{i+1}^{\mathrm{act}} = \mathbf{R} + \mathbf{R}_{i+1}^{\mathrm{vis}} . \tag{32}$$

The algorithms of computer simulation of viscoelastic deformations of thin inhomogeneous slabs will be presented as follows:

(1) with the aid of a graphical interface that implements the technique of visual object-oriented modeling [5], the assignment of the geometric configuration of the slab, of the physical properties (elasticity modulus, Poisson coefficient, parameters of the relaxation kernel) of its elements, boundary conditions, and of the acting external forces are made;

(2) according to the algorithm given in [6], the rigidity matrix $[\mathbf{K}^{\mathrm{gl}}]$ and the vector of nodal forces **R** are formed;

(3) the number of the step of the iteration process $i = 0$ is assigned as well as the time interval $t \in [t_0; t_N]$ over which the stressed–strained state of the viscoelastic slab is investigated;

(4) the boundary conditions are taken into account; for this purpose the correction of the matrix $[\mathbf{K}^{\mathrm{gl}}]$ and of the vector **R** is made. The correction of the matrix $[\mathbf{K}^{\mathrm{gl}}]$ results in the reduction of its dimensionality due to the elimination of the boundary values of displacements and moments, with the band and symmetric structures of the matrix not being disturbed. As a result, one obtains a new rigidity matrix $[\mathbf{K}^{\mathrm{gl}}]_i$, a new vector of nodal forces $\mathbf{R}_i^{\mathrm{act}}$ (with the assumption that $\mathbf{R}_i^{\mathrm{act}} = \mathbf{R}$ at the zero step of the iteration process), the vector of the unknown nodal displacements and

TABLE 1. Deflections at the Center of a Thin, Hinged Viscoelastic Slab

Time, days	Deflection from the action of a uniformly distributed loading with intensity q = 1000 Pa, cm			Deflection from the action of loading concentrated at the center P = 1000 Pa, cm		
	I	II	III	I	II	III
0	0.118	0.118	0.00	0.338	0.338	0.00
10	0.161	0.161	0.00	0.460	0.457	0.66
20	0.201	0.191	5.24	0.574	0.543	5.71
40	0.249	0.228	9.21	0.712	0.651	9.37
60	0.264	0.247	6.88	0.755	0.710	6.34
80	0.268	0.257	4.28	0.765	0.733	4.37
100	0.269	0.262	2.67	0.768	0.748	2.67
150	0.269	0.267	0.75	0.768	0.757	1.45

Note. I, solution according to [2]; II, solution by the proposed algorithm; III, relative error, %.

TABLE 2. Deflections at the Center of a Thin, Square, Fixed Viscoelastic Slab

Time, days	Deflection from the action of a uniformly distributed loading with intensity q = 1000 Pa, cm			Deflection from the action of loading concentrated at the center P = 1000 Pa, cm		
	I	II	III	I	II	III
0	0.037	0.037	0.00	0.163	0.163	0.00
10	0.050	0.050	0.00	0.222	0.222	0.00
20	0.062	0.061	1.64	0.277	0.264	4.92
40	0.077	0.071	8.45	0.344	0.315	9.21
60	0.082	0.077	6.49	0.364	0.347	4.90
80	0.083	0.080	3.75	0.369	0.355	3.94
100	0.083	0.082	1.22	0.371	0.362	2.49
150	0.083	0.083	0.00	0.371	0.368	0.82

Note. I, solution according to [8]; II, III, see the Note to Table 1.

moments $\mathbf{g}_i^{\mathrm{n}}$, the vector of known boundary displacements and moments $\mathbf{g}^{\mathrm{b}}$, and the vector of the numbers of boundary nodes;

(5) the Cholesky preconditioning [7] for the matrix $[\mathbf{K}^{\mathrm{gl}}]_i$ is made;

(6) the solution of the system of linear algebraic equations of the form of Eq. (31) is performed with the preconditioned matrix $[\mathbf{K}^{\mathrm{gl}}]_i$ by the method of conjugate gradients [7];

(7) for each finite element the vector $\mathbf{R}_{i+1}^{\mathrm{vis}}$ is calculated by Eq. (30) and then, using Eq. (32), the next vector $\mathbf{R}_{i+1}^{\mathrm{act}}$ is found. Here, for the finite elements that contain the boundary nodal points the known displacements $\mathbf{g}^{\mathrm{b}}$ are taken into account;

(8) the vector of nodal displacements $\mathbf{g}_i^{\mathrm{n}}$ found is preserved;

(9) the number of the iteration step is increased by unity, $i = i + 1$;

(10) if the current model time is inside the time interval considered, $t_{i+1} \in [t_0; T_N]$, passage to step 6 is made, otherwise — to step 11;

(11) visualization is made and the results of simulation are stored.

In order to check the adequacy of the mathematical model, to verify the algorithms and software, a number of problems had been considered for which exact solutions were found.

Using the Volterra principle, on the basis of the Navier solution it is possible to calculate a precise value of the deflection of a thin rectangular hinged viscoelastic slab under the action of uniformly distributed or concentrated vertical loading. For this purpose, in the elastic solution the elasticity modulus E and Poisson coefficient μ were replaced by constants G and K and then the constant G was replaced by the operator Γ [2]. Analogously, on the basis of solutions for different slabs — an elastic square slab fixed along the contour [8], a circular one fixed along the contour [2], a circular hinged one with a hole at its center [9] — deflections for the corresponding viscoelastic slabs have been found.

TABLE 3. Maximum Deflection of a Thin Circular Plate from the Action of Uniformly Distributed Load of Intensity q = 100,000 Pa

Time, days	Deflection at the center of a solid, fixed, circular slab, cm			Maximum deflection of a hinged circular slab with a hole, cm		
	I	II	III	IV	II	III
0	9.214	9.257	0.46	35.9	36.618	1.96
10	11.776	11.942	1.39	47.604	49.273	3.39
20	14.409	14.549	0.96	57.591	60.192	4.32
40	18.715	16.987	10.17	67.125	69.972	4.07
60	21.063	19.107	10.24	74.236	73.433	1.09
80	22.054	20.453	7.83	75.958	75.712	0.32
100	22.427	21.292	5.33	77.344	76.852	0.64
150	22.618	22.218	1.80	78.001	77.522	0.62
200	22.632	22.608	0.11	78.009	77.908	0.13

Note. I, II, III, see the Note to Table 1; IV, solution according to [9].

TABLE 4. Maximum Deflection of the Disk-Like Floor under Different Conditions of the Coupling of Its Elements

Conditions of coupling of the disk-floor elements	Solution by the proposed algorithm			Deflection according to experiment in [1], cm
	instantaneous deflection, cm	stabilizing deflection, cm	time of attainment of stabilizing deflection, days	
All seams are not monolithically connected	0.547	0.917	47	0.940
Seams between slabs are monolithically connected	0.292	0.337	23	0.340
All seams between slabs are monolithically connect	0.255	0.309	22	0.310
Solid disk-floor	0.011	0.014	12	—

Problem 1. A thin, homogeneous, square viscoelastic slab with side a = 1 m and thickness h = 0.01 m subjected to the action of a uniformly distributed loading of intensity q = 1000 Pa or a loading P = 1000 Pa concentrated at the center of the slab was considered. The relaxation kernel has the form of Eq. (15), where δ = 0.05 1/24 h, δ_1 = 0.05 1/24 h, E = 40, 000 MPa, and μ = 0.17. In solving the problem by the method of finite elements, the slab was discretized by 900 finite elements in the form of rectangles. The time step was selected equal to 12 h. The time of finding the solution over the interval from 0 to 150 days was of the order of 37 sec. The results of verification are given in Tables 1 and 2.

Problem 2. A thin, homogeneous, solid circular slab fixed along the contour [8] and a hinged, along the contour, slab with a hole of 6 mm at the center [9] were considered. The diameter of each of the slabs was taken equal to 12 m with the thickness h = 0.2. The slabs were subjected to a uniformly distributed vertical loading of intensity q = 100,000 Pa. The relaxation kernel has the form of Eq. (15), where δ = 0.035 1/24 h, δ_1 = 0.055 1/24 h, E = 30,000 MPa, and μ = 0.3. A fourth of the plate which had been discretized by 510 finite elements in the form of rectangles for a solid slab and 260 elements for the plate with holes was considered. The time step was selected equal to 12 h. The time of finding the solution in the interval from 0 to 150 days was of the order of 9 sec for the solid slab and about 1 sec for the slab with a hole. The results of the verification are given in Table 3.

Problem 3. A floor disk of the precast-monolithic frame of a building [1, 5] consisting of three multihollow slabs and crossbars was considered (see Fig. 1). The end faces of the slabs are joined in one plane by bearing and linking crossbars into a single disk. The corners of the extreme slabs are rigidly fixed. Acting on the slabs are their own weight and an external loading uniformly distributed over the middle slab of intensity q = 6000 Pa. The deflection of the disk depending on the conditions of the coupling of its elements was investigated:

(1) the slabs and bracing crossbars along their lengths are not interconnected;

(2) the slabs are connected along their lengths;

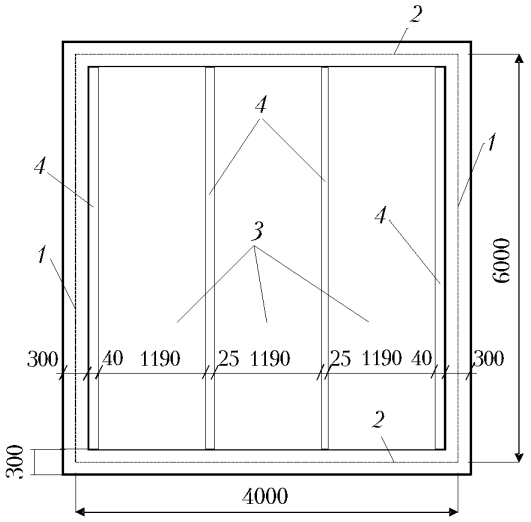

Fig. 1. Disk-like floor of the precast-monolithic frame of a building: 1) bracing crossbar; 2) bearing crossbar; 3) multivoid slabs; 4) seams (dimensions in mm).

(3) the slabs and braced crossbars are connected along their length;

(4) the solid slabs are connected among themselves and the bracing crossbars.

The relaxation core was adopted in the form of Eq. (15), where $\delta = 0.05\ 1/24$ h and $\delta_1 = 0.075\ 1/24$ h, the elasticity modulus for crossbars $E = 30{,}000$ MPa, for slabs $E = 20{,}000$ MPa, for the monolithic seams $E = 16{,}000$ MPa, and the Poisson coefficient $\mu = 0.2$. In modeling, the floor disk was considered as an inhomogeneous thin slab of variable thickness with through vertical holes. The length of the slab was taken equal to $a = 6.3$, the width — to $b = 4.3$. The through horizontal holes were excluded from consideration; where such holes were present the thickness of the slab was taken equal to the actual thickness of the concrete. A fourth of the floor disk which had been discretized by 1732 finite elements in the form of rectangles was considered. The time step was selected equal to 12 h. The time of finding a solution in the interval from 0 to 100 days was of the order of 91 sec.

The results of investigation of the mathematical model are presented in Table 4. For the considered floor disk with nonmonolithic seams all slabs and carrying crossbars develop deflection. The middle slab has a maximum deflection. The bracing crossbars are not deflected. With monolithically connected seams between the slabs the magnitude of deflection of the central slab decreases. The bracing crossbars do not deflect. In the case of all the seams being filled-joined, the magnitude of the deflection of the central slab decreases still further. The bracing crossbars are deflected. Provided the slabs are bulk-homogeneous, their deflection is minimal.

CONCLUSIONS

1. According to the results of simulation, the proposed mathematical model, algorithm and software may be used for investigation of viscoelastic deformation of inhomogeneous thin slabs. The relative error of the solutions found did not exceed 12%, which makes it possible to use the proposed mathematical model for solving practical problems.

2. For some materials, the magnitude of viscoelastic deformations may be comparable with the magnitude of instantaneous deformations (see Tables 1–3). Therefore, to ensure the reliability of the structures from such materials it is necessary to take viscoelastic deformations into account.

3. The advantage of the proposed mathematical model and the techniques of its investigation is the possibility of considering the stressed–strained state of in-plan inhomogeneous, or with through holes, viscoelastic thin slabs of complex geometry and with different boundary conditions by means of assigning various properties to each finite element that discretized a slab.

4. According to the adopted Kirchhoff hypothesis, for the discretization of slabs use was made of flat finite elements in the form of rectangles, through vertical holes being excluded from consideration. These two circumstances

made it possible to reduce the dimensionality of the rigidity matrix, which made it possible to considerably accelerate the process of finding instantaneous deformations.

5. In case of adoption of the hypothesis of the constancy in time of the Poisson coefficient μ and rigidity modulus E, the global matrix of rigidity at each step of the iteration process will remain unchanged. This assumption made it possible to considerably accelerate the process of finding a viscoelastic solution. For this purpose, at the zero iteration (in finding instantaneous deformations) one can somehow transform the matrix $[\mathbf{K}^{gl}]$: e.g., find the matrix $[\mathbf{K}^{gl}]^{-1}$ or expand it into the product of diagonal matrices $[\mathbf{K}^{gl}] = [\mathbf{L}][\mathbf{U}]$, where $[\mathbf{L}]$ is the lower triangular matrix; $[\mathbf{U}]$ is the upper triangular matrix, and at subsequent iterations use should be made of the already transformed matrix $[\mathbf{K}^{gl}]$. But a computational experiment has shown that this requires greater time expenditures than the application of the method of conjugate gradients with the preconditioned matrix $[\mathbf{K}^{gl}]$. The preconditioning of the matrix of the system is made once at the zero iteration. Moreover, in order to accelerate the iteration process, in the method of conjugate gradients one can select the solution obtained at the previous step as the initial approximation. Thus, the time spent to find deformations at any step of the iteration process turned out to be much smaller than the time needed to fulfill the zero iteration, i.e., to find instantaneous deformations.

NOTATION

a, length of the slab, m; $[\mathbf{B}]$, coordinate matrix; b, width of the slab, m; E, elasticity modulus, Pa; G, shear modulus, Pa; $\mathbf{g}$, vector of displacements and moments of an arbitrary point of a finite element; $\mathbf{g}^{b}$, vector of the known boundary displacements and moments; $\mathbf{g}^{n}$, vector of the displacements and moments of the finite-element nodes; h, thickness of a slab, m; K, module of volumetric deformation, Pa; $[\mathbf{K}]$, local rigidity matrix of one finite element; $[\mathbf{K}^{gl}]$, global rigidity matrix of the entire structure (slab) as a whole; K_{kl}^{gl} and K_{kl}^{r}, elements of the global and r local rigidity matrices of the element that characterize the contribution of the lth single displacement to the kth component of nodal forces, $k = 1, 4$, $l = 1, 4$; N, number of finite elements used for discretization of the slab considered; P, concentrated force, N; q, intensity of uniformly distributed loading, Pa; $\mathbf{R}$, vector of nodal forces acting on a finite element; $\mathbf{R}_{i+1}^{act}$, vector of actual nodal forces at the instant of time t_{i+1}; $\mathbf{R}_{i+1}^{vis}$, vector of additional nodal forces acting on a finite element and accounting for the viscoelastic properties of material by the instant of time t_{i+1}; r, number of the local rigidity matrix; t, time, sec; U, energy of deformation of a finite element, J; u, displacement along the X axis, m; u_0, displacement of the points of the middle plane along the X axis (0 is the plane of the slab at $z = 0$), m; V, volume of a finite element, m^3; v, displacement along the Y axis, m; v_0, displacement of the points of the middle plane along the Y axis (0 is the plane of the slab at $z = 0$), m; w, displacement along the Z axis (deflection), m; x, y, z, coordinates of the point of the slab; $\boldsymbol{\alpha}$, vector of unknown coefficients in expansion of the function of deflections over powers x and y; Γ_{vol} and Γ_{sh}, operators of volumetric and shear relaxations; $\Gamma_{vol}(t, \xi)$ and $\Gamma_{sh}(t, \xi)$, kernels of volumetric and shear relaxations; γ_{xy}, shear deformations in the XY plane; δ and δ_1, relaxation parameters calculated and found experimentally, respectively, sec^{-1}; $\boldsymbol{\varepsilon}$, vector of deformations; $\boldsymbol{\varepsilon}_{i+1}$, vector of deformations at the instant of time t_{i+1}; ε_{int}, intensity of deformations; ε_x, ε_y, ε_z, deformations along the X, Y, Z axes; ε_{av}, average deformations; θ_x and θ_y, angles of slab rotation relative to the X and Y axes; μ, Poisson coefficient; σ, vector of stresses; σ_{i+1}, vector of stresses at time t_{i+1}; σ_{int}, intensity of stresses; σ_x, σ_y, σ_z, normal stresses along axes X, Y, Z; τ_{xy}, shear stresses in the XY plane; ξ, integration variable. Subscripts and superscripts: act, actual; av, average value; b, boundary of considered slab; gl, global; i, number of the step of an iteration process; j, number of the time interval considered; int, intensity of stresses or deformations; n, nodes of a finite element; sh, shear; tr, transposition of a matrix or vector; vis, viscoelastic; vol, volumetric; 0, middle layer of the slab.

REFERENCES

1. V. E. Bykhovtsev, A. V. Bykhovtsev, and V. V. Bondareva, *Computer Modeling of the Systems of the Nonlinear Mechanics of Grounds* [in Russian], Gomel' F. Skorina Gos. Univ., Gomel' (2002).
2. E. I. Starovoitov, *Principles of the Theory of Elasticity*, *Plasticity*, *and Viscoelasticity*, *Textbook for Building Specialists of Higher Educational Establishments* [in Russian], Belorus. Gos. Univ. Transporta, Gomel' (2001).
3. N. A. Tsytovich, *Mechanics of Grounds* [in Russian], Stroiizdat, Moscow (1982).

4. O. Zenkevich, *Method of Finite Elements in Engineering* [Russian translation], Mir, Moscow (1975).
5. V. E. Bykhovtsev, A. V. Bykhovtsev, and K. S. Kurochka, Visual object-orientated modeling of buildings with foundations on ground bases, in: *Proc. Int. Sci.-Tech. Conf.* [in Russian], 10–12 October 2001, Vol. 2, Minsk (2001), pp. 5–16.
6. K. S. Kurochka, Numerical simulation of deformations of a bulk fragment of a carcass building, *Mat.–Technol.–Instrum.*, **7**, No. 3, 29–32 (2002).
7. A. A. Samarskii and A. V. Gulin, *Numerical Methods: Textbook for Higher Educational Establishments* [in Russian], Nauka, Moscow (1989).
8. S. P. Timoshenko and C. Voinovsky-Kriger (G. S. Shapiro, Ed.), *Theory of Plates and Shells* [Russian translation], GIFML, Moscow (1963).
9. V. A. Gastev, *A Brief Course in the Resistance of Materials* [in Russian], Nauka, Moscow (1977).